

AUTOMATING SNAKES FOR MULTIPLE OBJECTS DETECTION

Anonymous ACCV submission

Paper ID 329

Abstract. Active contour or snake has emerged as an indispensable interactive image segmentation tool in various applications. However, snake fails to serve many significant image segmentation applications that require complete automation. Here, we present a novel technique to automate snake/active contour for multiple objects detection. We first apply a probabilistic quad tree based approximate segmentation technique to find the regions of interest (ROI) in an image, evolve modified GVF snakes within ROIs and finally classify the snakes into object and non-object classes using boosting. We propose a novel loss function for boosting that is more robust to outliers concerning snake classification and we derive a modified Adaboost algorithm by minimizing the proposed loss function to achieve better classification results. Extensive experiments have been carried out on two datasets: one has importance in oil sand mining industry and the other one is significant in bio-medical engineering. Performances of proposed snake validation have been compared with competitive methods. Results show that proposed algorithm is computationally less expensive and can delineate objects up to 30% more accurately as well as precisely.

1 Introduction

Snake/active contour [2] has made its recognition as an interactive image segmentation tool for the last two decades. However, it is yet to be seen as a completely automated segmentation tool. Snake algorithms consist of three sequential steps: snake initialization, snake evolution and snake validation [3]. For multiple objects detection, seeds are chosen inside the objects at the initialization step, then snakes are evolved from those seed points and finally the evolved snakes are passed through a validation procedure to examine whether the snakes delineate the desired objects [3]. Substantial endeavors have taken place on the initialization and evolution steps towards snake automation. Most of the existing initialization algorithms [4] exploit the local maxima or other characteristics of the external energy that help to generate seed points within the objects. However, clutters in the noisy and poorly illuminated images generate considerable amount of seed points and snakes evolved from those seeds do not converge to the object boundaries. This necessitates a good validation scheme after snake evolution. Unfortunately, the validation step has not received much attention till date.

40 Saha *et al.* [3] proposed a snake validation scheme using principal compo-
41 nent analysis (PCA). Their method places seeds blindly on the entire image
42 and evolve one snake from each seed. When all snakes converge, a pattern im-
43 age (an annular band) is formed across each snake contour. Each pattern image
44 is then projected into an already trained PC (principal component) space and
45 PCA reconstruction error is computed. The snakes associated with lower recon-
46 struction errors than a threshold are considered as objects. Pattern images bear
47 information regarding bright-to-dark (or vice-versa) transition across the object
48 contours and show good discrimination capability between object and non-object
49 classes. This validation technique is effective when the gradient strength of ob-
50 ject boundaries is considerably high. Besides, throwing a large number of seeds
51 blindly over an entire image might not be feasible for some applications, since
52 the snake evolution can be computationally expensive. Thus, a handful of crucial
53 seed points are always helpful.

54 In this paper, we propose a probabilistic quad tree (QT) based snake initial-
55 ization scheme which is computationally inexpensive. QT automatically seeks
56 ROIs from an image where the probabilities of locating objects are very high.
57 We throw seeds only within ROIs and evolve one modified Gradient Vector Flow
58 (GVF) snake [5] from each seed. Then we validate each evolved snake to verify
59 whether they belong to object or non-object class. During validation, each snake
60 is passed through a strong classifier formed by Adaboost [6]. We classify snake
61 contours into objects and non-objects based on a set of features and we apply
62 Adaboost for selecting important features. The parameters of the adaboost algo-
63 rithm are estimated by minimizing an exponential loss function. Here, it is noted
64 that one shortcoming of the exponential loss function associated with Adaboost
65 algorithm is that the penalty increases exponentially negative margins which
66 incurs high misclassification error rates due to outliers [6]. We propose a novel
67 loss function that incurs smaller penalties in the negative margin, and thus make
68 Adaboost more robust to outliers. Also, we can choose the amount of penalty ju-
69 diciously from the training set using cross validation. We exploit the advantages
70 of multiple features including region, edge and shape over PCA-based intensity
71 feature proposed earlier [3]. Note that our proposed initialization and validation
72 algorithm could be successfully used as plugins with any existing snake evolution
73 techniques. We have carried out experiments on two real datasets: (a) oil sand
74 mining images [5]: analyzing these images help to improve the performance of
75 oil sand extraction process and (b) leukocyte images [7]: processing these images
76 help in the study of inflammation as well as in the design of anti/pro inflamma-
77 tory drugs. Results illustrate that our proposed algorithm is faster, more reliable
78 and robust than competitive methods.

79 The organization of this paper is as follows. Section 2 discusses proposed quad
80 tree based snake initialization technique. Section 3 elaborates snake validation
81 using boosting and illustrates proposed regularization into boosting framework.
82 Section 4 demonstrates the performances of proposed techniques and displays
83 comparative analysis of proposed techniques with competitive methods. Section 5

84 concludes our proposed work. Appendix includes derivation of proposed discrete
85 Adaboost algorithm.

86 2 Quad tree based snake initialization

87 Quad tree [8] based segmentation algorithm receives an image as an input, and
88 then divides it into four adjacent, non-overlapping quadrants if it meets pre-
89 specified criteria, subsequently each quadrant is divided similarly and the pro-
90 cess proceeds iteratively until it fails the pre-defined criteria. Consequently, the
91 algorithm locates objects by smaller rectangular boxes. In our application here,
92 the QT algorithm computes a posterior probability and splits the current region
93 into four quadrants if the value of the posterior probability is between two pre-
94 determined thresholds. If the value of the posterior probability is greater than
95 the upper threshold then the region is likely to contain objects ; if it is less than
96 the lower threshold then it is likely to contain background. We locate objects
97 by finding homogeneous regions based on local brightness and texture proper-
98 ties. We compute the posterior probability of a region (O) being object/non-
99 object: $P(O/T, B) \propto P(T/O)P(B/O)P(O)$, where $P(O)$ is the prior probabil-
100 ity. $P(T/O)$ and $P(B/O)$ are the likelihood of the region regarding texture and
101 brightness respectively. Proposed probabilistic QT algorithm converges faster
102 and delineates objects more accurately than deterministic quad tree algorithm if
103 a suitable, application specific prior can be chosen. We compute texture energy
104 (T) by the response of Gabor filters [8] and brightness (B) by the maximum
105 singular value decomposition (SVD) [9] of the region. Maximum SVD encodes
106 average brightness and Gabor filter response represents discriminative texture
107 information for the objects. The details of computing posterior probability and
108 two thresholds are mentioned in section 4.

109 3 Snake validation using boosting

110 We compute different features for each converged snake contour, such as, con-
111 tour shape features (form factor, convexity, extent, modification ratio [10] etc.),
112 regional features (intra and inter class variance, entropy etc.), and edge based
113 features (GICOV [7], gradient strength etc.) for snake validation. We use Ad-
114 aboost (variant of boosting) for selecting important features. At the training
115 phase, boosting picks only important features for snake validation from a set
116 of features computed on training snake contours and finds the weights associ-
117 ated with those features. We place seeds blindly over the training images and
118 evolve one snake from each seed and classify the snakes as objects manually that
119 converge at object contours found on the ground truth made by the experts; oth-
120 erwise consider the snakes as non-objects and thus form a training set consisting
121 of both positive (object) and negative (background) samples. The Adaboost al-
122 gorithm forms a strong classifier by combining a set of weak learners linearly in
123 an iterative manner [6]. We use decision stump (threshold) [6] as weak classifier.
124 Decision stump is a single level decision tree. Decision stump, $G_j(x)$ for feature

125 f_j is defined as, $G_j(x) = 1$ if $x_j > \theta_j$, otherwise, $G_j(x) = 0$, where θ_j is some fea-
 126 ture value of x_j chosen as threshold and $x = [x_1, x_2, x_3, \dots, x_j, \dots, x_n]$ is the feature
 127 set. Finding the best decision stump at each stage is similar to learning a node in
 128 a decision tree. We search over all possible features $x = [x_1, x_2, x_3, \dots, x_n]$ and
 129 for each feature, we search over all possible thresholds θ induced by sorting the
 130 observed values of x and pick x_k with θ_k that gives lowest misclassification error
 131 among all given features during training. At test phase, proposed QT algorithm
 132 discussed in section 2 locates ROIs (rectangular regions/patches) over the test
 133 images where the probability of localizing objects is greater than a predeter-
 134 mined upper threshold. We place seeds only within ROIs and grow one snake
 135 from each seed. When all snakes are fully converged, we compute the values
 136 of the important features for each snake and multiply them with the weights
 137 associated with the features chosen by boosting during training phase and sub-
 138 sequently add them to form a strong classifier, $G(x) = \text{sign}(\sum_{m=1}^M \alpha_m G_m(x))$,
 139 where, α_m is the weight associated with weak classifier $G_m(x)$. If the sign of the
 140 response of the strong classifier for a snake contour is positive then it is classified
 141 into object class, otherwise it is classified into non-object class. For classification,
 142 Adaboost minimizes an exponential loss function: where y is the response and f
 143 is the prediction. The drawback of this exponential loss function is that it incurs
 144 substantial misclassification error rate as the penalty increases exponentially for
 145 large increasing negative margin due to outliers [6]. To address this problem, we
 146 propose a novel loss function: $L(y, f(x)) = \exp(-yf(x) + \lambda|y - G(x)|)$, where
 147 $\lambda < 0$ and $G(x)$ is the prediction of the weak classifier chosen at the current
 148 stage. We have mainly incorporated one extra term in the existing exponential
 149 loss function that acts as a regularizer. At any boosting iteration, the proposed
 150 loss function is the same as the existing loss function if the misclassification er-
 151 ror rate at current stage is zero (proposed term vanishes when $\lambda = 0$). The only
 152 difference between the proposed and the exponential loss function is that the
 153 penalty associated with the proposed loss function is less than that of the expo-
 154 nential one, if the misclassification error rate at current stage is not equal to zero
 155 (shown in Fig.1(a) where loss is plotted against a function of the classification
 156 margin $y.f$). This modification leads to a low misclassification error rate and it
 157 becomes more robust to outliers. One additional advantage of this proposed loss
 158 function is that the user can adjust the amount of penalty for negative margins
 159 after observing the classifier performance over a training data set. Accordingly,
 160 we determine the value of λ through cross validation (λ is a function of k shown
 161 in the appendix and the value of k is determined experimentally). We derive
 162 a modified Adaboost algorithm by minimizing the proposed loss function (The
 163 derivation is shown in Appendix).

164 Our modified Adaboost finds the feature weight, $\alpha_m = \log(k(1-err_m)/err_m)$,
 165 $k \geq 1$, where, for the existing Adaboost algorithm the value of k is always 1. This
 166 leads to the weights associated with misclassified observations at any stage is k
 167 times as much as the existing Adaboost (derivation is shown in the Appendix).
 168 The value of k for our modified Adaboost is determined by cross-validation and
 169 is discussed in the next section.

170 Our proposed term in the existing loss function acts as a regularizer in the
 171 boosting framework. There are two well known regularized boosting algorithms,
 172 ϵ -boosting [6] and l_1 - regularized boosting [11] available in the literature. Unlike
 173 other two methods, our method can adaptively adjust the effects of regularization
 174 in the boosting framework by selecting the proper value of k from the training
 175 data set. The regularization strategy in ϵ - boosting is imposed through shrinking
 176 the contribution of each feature (feature weight). In l_1 - regularized boosting, the
 177 exponential loss function is minimized with l_1 - regularization. This provides
 178 sparse solution and acts as a regularizer.

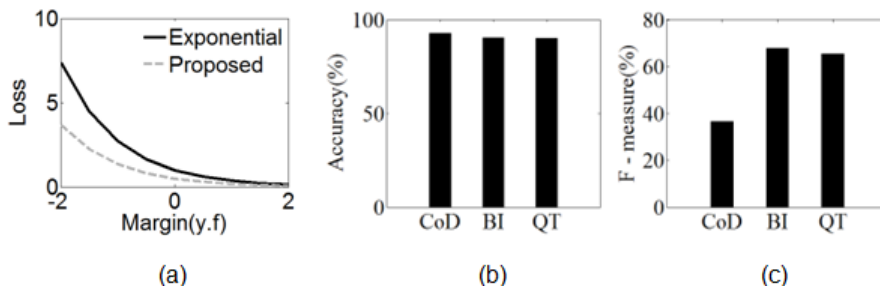


Fig. 1. (a) Loss functions for two class classification. (b) Accuracy and (c) F-measure for three different snake initialization methods.

179 **4 Results and Discussions**

180 We have carried out experiments on two real data sets: oil sand images and
 181 leukocyte microscopy images.

182 **4.1 Oil Sand Images**

183 In the oil sand extraction process, oil sand ore is crushed, broken into smaller
 184 particles through crusher and then passed through screens to reject oversize
 185 ores and the undersize ores are transported to hydrotransport plant for fur-
 186 ther processing. Here, ore size is an important measure to estimate crusher as
 187 well as screen efficiency. Towards achieving this goal, oil sand images are cap-
 188 tured through camera mounted over conveyor belt before and after the crusher
 189 as well as screen. Oil sand particles are detected in the images using the pro-
 190 posed method and then the particle size distribution (PSD) is computed. PSD
 191 is a histogram showing frequency of the particles over their sizes. In this pa-
 192 per, we have concentrated on the automatic detection of the oil sand parti-
 193 cles. We construct a training set using 20 images and test set using 100 im-
 194 ages sampled randomly from an online video of oil sand particles over con-
 195 veyor belt. For QT based snake initialization, we find the distribution for prior

196 and likelihood as well as the two threshold values (P_{th1} and P_{th2}) of the
 197 posterior probability ($P(O/T, B)$) experimentally from the training set. We
 198 have $P(O/T, B) \propto P(T/O)P(B/O)P(O)$, where T and B represent texture
 199 and brightness respectively. Maximum Singular Value Decomposition (SVD) en-
 200 codes average brightness of a region where average of the response of the gabor
 201 filter on a region encodes texture of the region. Experimentally it is found
 202 that maximum SVD of the oil sand patch follows doubly truncated exponential
 203 (DTE) distribution. Probability density function (pdf) of DTE [12] is given by,
 204 $P(B) = \frac{\exp(-(B-\mu)/\sigma)}{\sigma[1-\exp(-(x_0-\mu)/\sigma)]} I_{[\mu, x_0]}(B), \mu \leq B \leq x_0$. On the otherhand, the re-
 205 sponse of the gabor filter follows doubly truncated normal distribution (DTN);
 206 pdf of DTN is given by, $P(T) = \frac{\frac{1}{\sigma\sqrt{2\pi}}\exp(-(T-\mu)^2/2\sigma^2)}{\Phi(\frac{b-\mu}{\sigma})-\Phi(\frac{a-\mu}{\sigma})} I_{[a,b]}(T), a \leq T \leq b$, where
 207 Φ is the standard normal cumulative density function(cdf) [12]. The value of in-
 208 dicator function, $I_{[a,b]} = 1$ if $a \leq T \leq b$, and is 0 otherwise. $I_{[\mu, x_0]}(B)$ is defined
 209 similarly. A region will have high oil sand particles density if $P(O/T, B) \geq P_{th2}$.
 210 The two threshold values of the posterior probability (P_{th1} and P_{th2}) are deter-
 211 mined experimentally from the training set. The parameters of the above dis-
 212 tributions are estimated using maximum likelihood estimation (MLE). Fig. 2(a)
 213 and fig. 2(b) shows the distribution of the brightness and texture of the oil sand
 214 particles respectively.

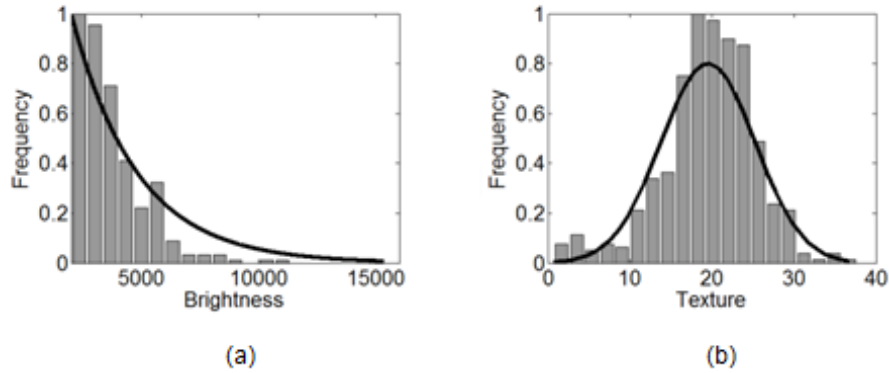


Fig. 2. Histogram of brightness and texture of oil sand particles.

215 Regions of Interest (ROI) generated by QT and seeds generated by Center
 216 of Divergence (CoD) [4] method are shown in Fig. 4. Table 1 illustrates the
 217 number of seeds generated by the proposed QT, CoD and blind initialization
 218 (BI) [3]. CoD refers to the local maxima of the external Gradient Vector Flow
 219 (GVF) field. The point from which the GVF vectors to all of its neighboring
 220 pixels radiate is considered as CoD. CoD is supposed to be located within the
 221 object and the snake evolved from CoD converges to the actual boundary of the

Table 1. Comparison among three snake initialization techniques.

Datasets	# of objects	# of seeds generated by		
		CoD	BI	QT
Oil Sand	349	3786	3000	686
Leukocyte	193	2402	4375	799

222 object in noise-free settings. Fig. 1(b) and 1(c) show accuracy and F-measure for
 223 CoD, BI and QT techniques with proposed modified Adaboost based validation
 224 technique respectively. F-measure combines both recall and precision into a single
 225 entity [13]. Results show that though all techniques possess the same accuracy,
 226 both BI and QT achieve 30% more F-measure value than that of CoD but QT
 227 generates significantly fewer seeds (Table 1) than other competitive methods.

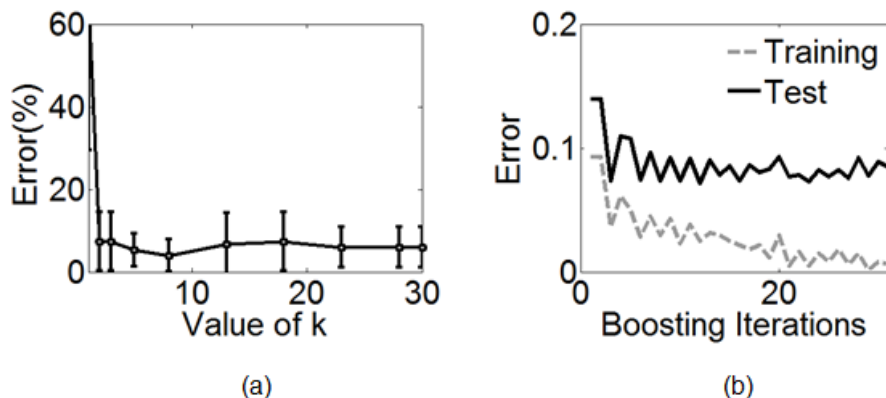


Fig. 3. (a) fivefold cross validation curve with standard error bars; the curve has minima at $k = 8$. (b) Misclassification error rate over the number of iterations for oil sand images.

228 Next, we determine the value of k (discussed regarding feature weight in
 229 section 3) using five-fold cross validation [6] technique. We compute misclassifi-
 230 cation errors for different values of k and is shown in Fig. 3(a). Standard error
 231 bars indicate the standard errors of the individual misclassification error rates
 232 for each of the five parts. It is observed that both the average misclassification
 233 error rate and standard error is minimum for $k = 8$ for oil sand images. For
 234 existing Adaboost algorithm, the value of k is always 1. Modified Adaboost al-
 235 ways outperforms the existing Adaboost algorithm because the modified one can
 236 select the best value of k for which the misclassification error is minimum. The
 237 misclassification error rate for boosting with decision stumps [6], as a function
 238 of the number of iterations for $k = 8$ is shown in Fig. 3(b).

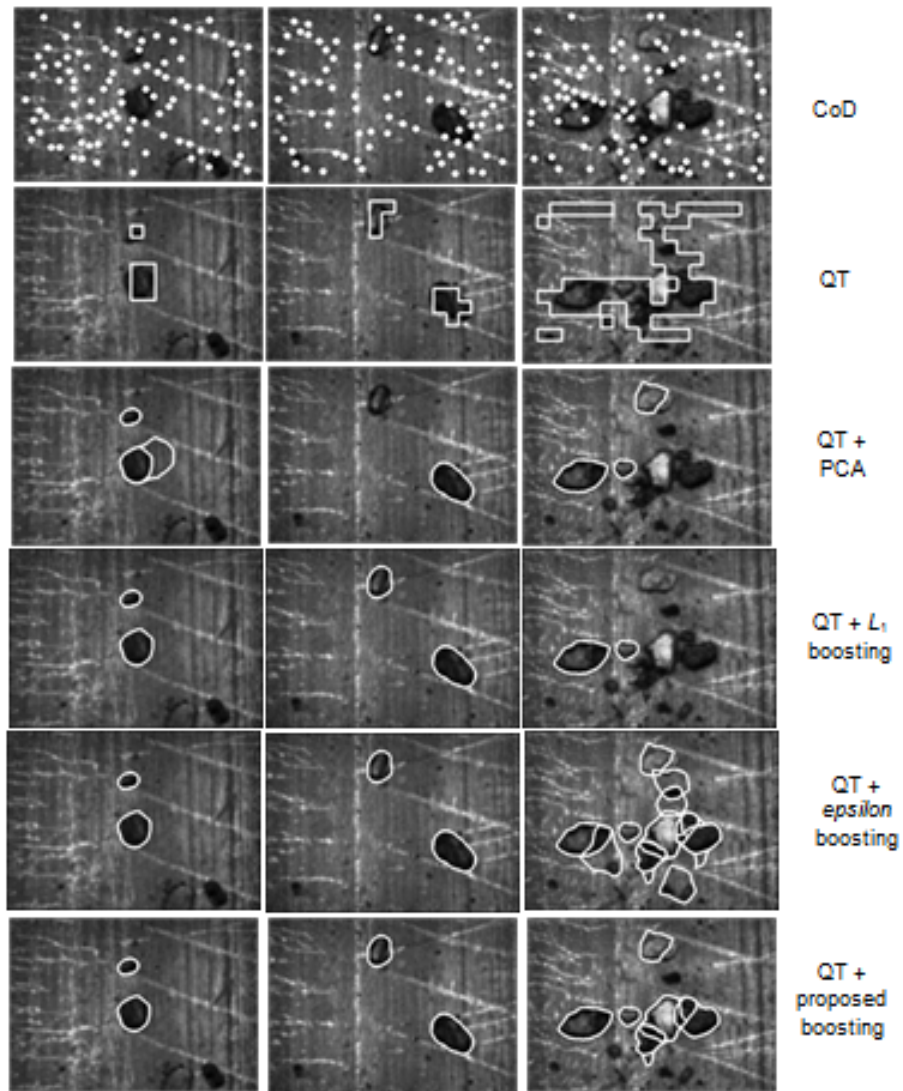


Fig. 4. Results of different methods on oil sand images.

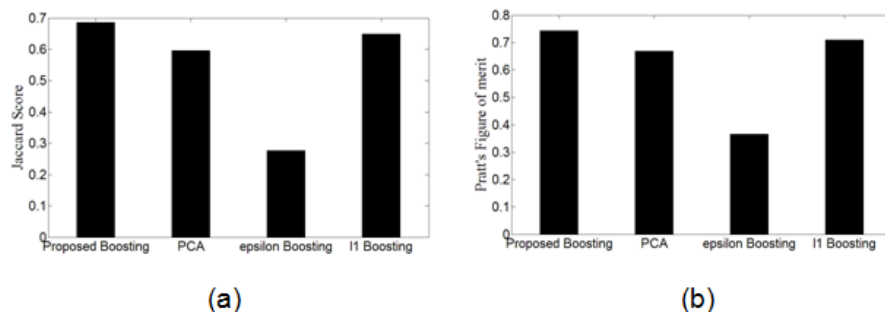


Fig. 5. Segmentation scores: (a) Jaccard Score and (b) Pratt's Figure of Merit of different methods on oil sand images.

239 Fig. 4 shows the results of proposed Adaboost, ϵ -boosting [6], l_1 regularized
 240 boosting [11] and PCA [3] on oil sand images and their comparisons are shown in
 241 Fig. 5 and Fig. 8(a). Fig. 5(a) shows the average Jaccard Score [1] and Fig. 5(b)
 242 shows the average Pratt's figure of merit (PFOM) [14] for these methods. Jaccard
 243 Score measures the fraction of overlap area among detected and true objects.
 244 Pratt's figure of merit determines the closeness among detected and actual edge
 245 pixels. Domain expert visually determines actual edge pixels and true object area
 246 from an image. Both Jaccard Score and Pratt's figure of merit are important to
 247 judge the segmentation quality of an algorithm and both are bounded by 0 and 1.
 248 Superior performance of a segmentation algorithm is indicated by higher PFOM
 249 as well as Jaccard Score values.

250 4.2 Leukocyte Images

251 Leukocyte plays an important role in the study of inflammation. Inflammation
 252 is a natural defense mechanism initiated by tissue damage. During inflamma-
 253 tory responses, endothelium cell is activated, then leukocyte starts deviating
 254 from mainstream blood flow and contact the activated endothelium cell. This
 255 slowdown movement of leukocyte in contact with endothelium cell is known as
 256 rolling. Finally, from the rolling stage, leukocyte diffuses through the vascular
 257 wall, reach the injured tissues, and encounter the germs. Although inflammation
 258 is a normal defense mechanism, it sometimes becomes dangerous in the context
 259 of various inflammatory diseases. To combat such diseases, anti-inflammatory
 260 drugs are developed by blocking or controlling any of the necessary processes of
 261 inflammatory response. Here, the rolling velocity of leukocyte is an important
 262 factor in the study of inflammation. To measure and analyze the rolling velocity
 263 of leukocyte from the *in vivo* experiments, video recordings of the postcapillary
 264 venule of a cremaster muscle are made through a CCD camera coupled with the
 265 intravital microscope. Then leukocyte cells are detected from the video frames
 266 using the proposed method and a correspondence analysis is carried out be-

267 tween consecutive images and finally cell motility is measured [7]. In this paper,
 268 we have concentrated only leukocyte detection. We have carried out experiment
 269 on a training set of 5 and a test set of 25 leukocyte images. Detections obtained
 270 by proposed Adaboost, ϵ -boosting [6], l_1 regularized boosting [11] and PCA [3]
 271 techniques are shown in Fig. 6 and their comparisons are shown in Fig. 7 and
 272 Fig. 8(b).

273 4.3 Interpretation of Results

274 One can interpret that proposed adaboost based validation is better than ϵ -
 275 boosting [6], l_1 regularized boosting [11] and PCA [3] based technique since
 276 it can detect more oil sand particles and leukocytes accurately and precisely.
 277 Segmentation score (Jaccard Score and Pratt's Figure of Merit) as well as area
 278 under ROC curve of proposed adaboost is greater than that of other methods.

279 5 Conclusion and Fututre works

280 Towards complete automation of snake algorithm, we have proposed an initializa-
 281 tion as well as validation algorithm that could be utilized as a successful plug-in
 282 for existing snake/active contour tools. Existing research mainly focuses on the
 283 snake initialization and evolution steps and ignores the validation step. Here, we
 284 emphasize that we cannot omit the validation step in spite of applying the smart
 285 initialization technique of snake algorithm used for multiple objects detection.
 286 We have proposed probabilistic quad tree based approximate segmentation for
 287 snake initialization. We show that our proposed initialization outperforms ex-
 288 isting initialization methods. We have successfully incorporated regularization
 289 into boosting framework and we demonstrate that our intended loss function is
 290 more robust to outliers concerning snake classification into object and non-object
 291 classes. We also show that proposed boosting based snake validation technique
 292 outperforms existing PCA based validation method. Results of extensive exper-
 293 iments illustrate that proposed method is fast, reliable and more accurate than
 294 existing methods.

295 We would like to incorporate our initialization and validation methods with
 296 other well known snake evolution methods. Also we will further explore the
 297 characteristics of proposed regularization into boosting frameworks extensively
 298 by conducting experiments with available benchmark datasets.

299 6 Appendix

300 Derivation of Proposed Discrete Adaboost Algorithm

301

302 Proposed loss function is: $L(y, f(x)) = \exp(-yf(x) + \lambda|y - G(x)|)$, where $\lambda < 0$.
 303 Let $f_m(x) = f_{m-1}(x) + \beta_m G_m(x)$ be the strong classifier composed of first m
 304 classifiers. We can pose m -th iteration of adaboost as the following optimiza-
 305 tion, $(\beta_m, G_m) = \underset{\beta, G}{\operatorname{argmin}} \sum_{i=1}^N \exp[-y_i(f_{m-1}(x_i) + \beta G(x_i)) + \lambda|y_i - G(x_i)|]$

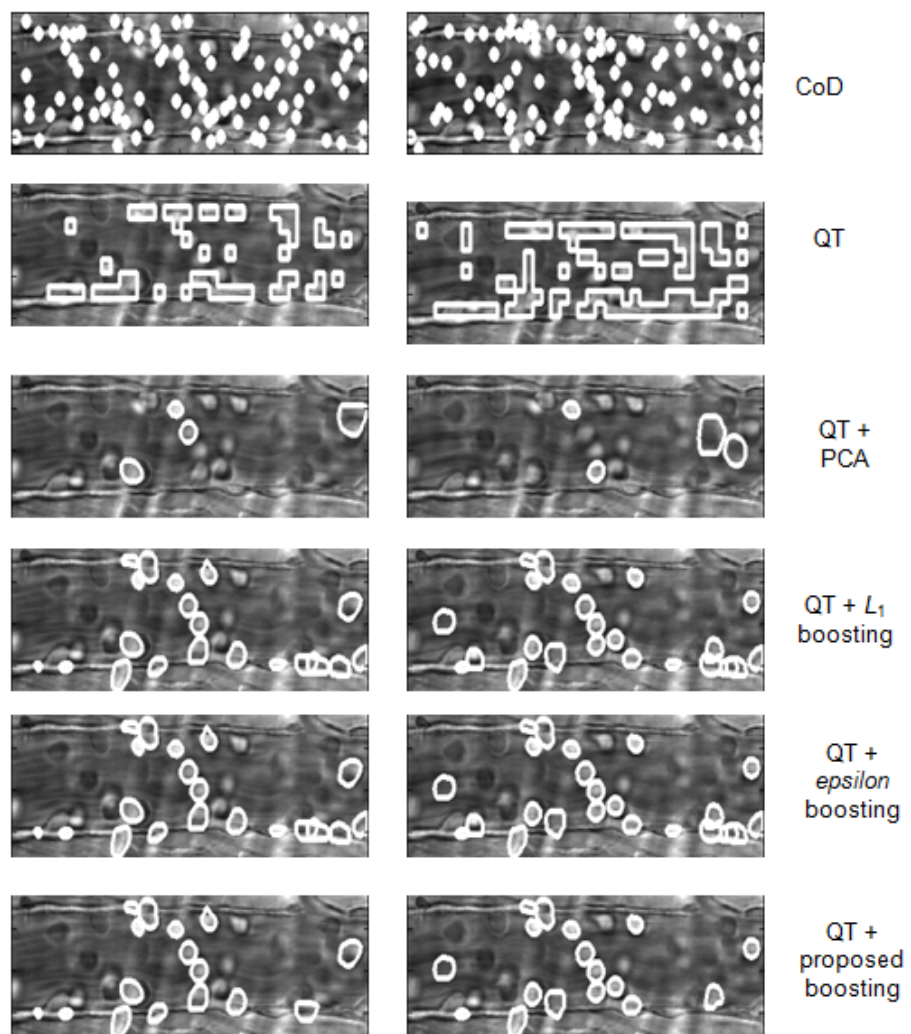


Fig. 6. Results of different techniques on on leukocyte images.

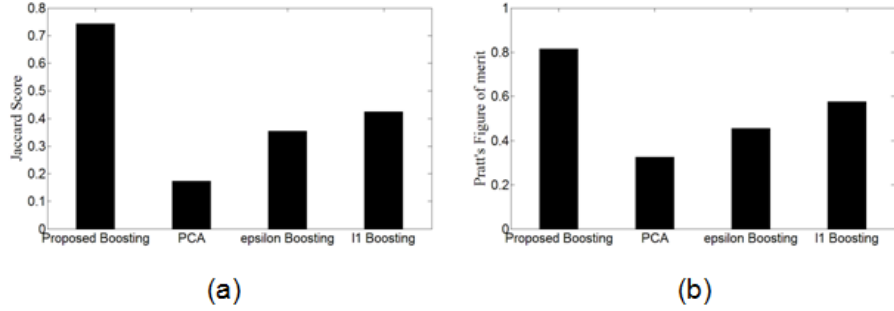


Fig. 7. Segmentation scores: (a) Jaccard Score and (b) Pratt's Figure of Merit of different methods on leukocyte images.

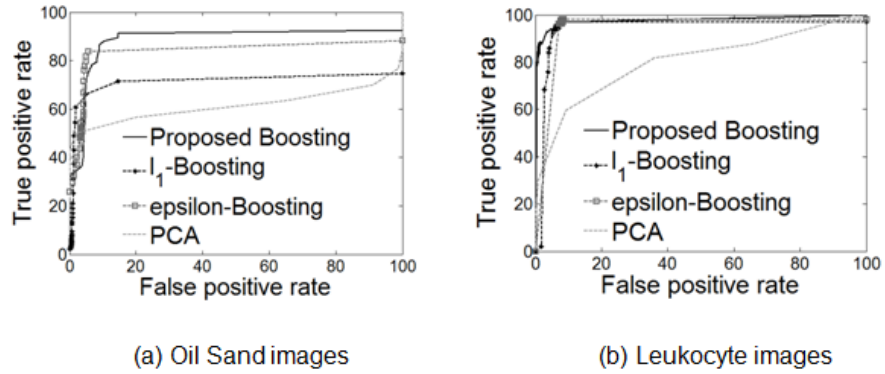


Fig. 8. Receiver Operating Characteristic (ROC) curves.

306 $\Rightarrow (\beta_m, G_m) = \underset{\beta, G}{\operatorname{argmin}} \sum_{i=1}^N w_i^m \exp[-y_i \beta G(x_i)] + \lambda |y_i - G(x_i)|$ where, $w_i^m =$
 307 $\exp(-y_i f_{m-1}(x_i))$ is free of both β and $G(x)$.
 308 $\Rightarrow (\beta_m, G_m) = \underset{\beta, G}{\operatorname{argmin}} [\exp(-\beta) \sum_{i: y_i = G(x_i)} w_i^m + \exp(\beta + 2\lambda) \sum_{i: y_i \neq G(x_i)} w_i^m]$.
 309 $= \underset{\beta, G}{\operatorname{argmin}} [\exp(\beta + 2\lambda) - \exp(-\beta)] \sum_{i: y_i \neq G(x_i)} w_i^m + \exp(-\beta) \sum_{i=1}^N w_i^m]$. The so-
 310 lution for β_m and G_m can be obtained in two steps. First, for any value of $\beta > 0$,
 311 the solution for G_m is: $G_m = \underset{G}{\operatorname{argmin}} \sum_{i=1}^N w_i^m I(y_i \neq G(x_i))$. Let $\operatorname{err}_m =$
 312 $\underset{G}{\operatorname{argmin}} \sum_{i=1}^N w_i^m I(y_i \neq G(x_i)) / \sum_{i=1}^N w_i^m$, then $\beta_m = \frac{\partial}{\partial \beta} (\sum_{i=1}^N w_i^m ((\exp(\beta +$
 313 $2\lambda) - \exp(-\beta)) \operatorname{err}_m + \exp(-\beta)) = 0 \Rightarrow \beta_m = \frac{1}{2} (\log \frac{1 - \operatorname{err}_m}{\operatorname{err}_m}) - \lambda = \frac{1}{2} (\log k \frac{1 - \operatorname{err}_m}{\operatorname{err}_m})$,
 314 where, $\lambda = -\frac{1}{2} \log(k)$, $k > 0$. Now, $w_i^{m+1} = w_i^m \exp(-\beta_m y_i G_m(x_i))$. Using the
 315 fact that $-y_i G_m(x_i) = 2I(y_i \neq G(x_i)) - 1$, we get, $w_i^{m+1} = w_i^m \exp(\alpha_m I(y_i \neq$
 316 $G(x_i))) \exp(-\beta_m)$ where, $\alpha_m = 2\beta_m = \log(k((1 - \operatorname{err}_m)/\operatorname{err}_m))$. So, $w_i^{m+1} =$
 317 $w_i^m \exp(\alpha_m I(y_i \neq G(x_i)))$. The factor $\exp(-\beta_m)$ multiplies all weights by the
 318 same value, so it has no effect.

319 References

- 320 1. Jaccard, P.: Distribution de la flore alpine dans le bassin des dranses et dans
 321 quelques rgions voisines. Bulletin de la Socit Vaudoise des Sciences Naturelles **37**
 322 (1901) 241–272
- 323 2. M. Kass, A.W., Terzopoulos: Snakes: active contour models. IJCV **1** (1987) 321–
 324 331
- 325 3. B. N. Saha, N.R., Zhang, H.: Snake validation: A pca-based outlier detection
 326 method. IEEE Signal Processing Letters **16** (2009) 549–552
- 327 4. Ge, X., Tian, J.: An automatic active contour model for multiple objects. ICPR
 328 **2** (2002) 881–884
- 329 5. B. N. Saha, N.R., Zhang, H.: Computing oil sand particle size distribution by
 330 snake-pca algorithm. ICASSP (2008) 977–980
- 331 6. T. Hastie, R.T., Friedman, J.: The elements of statistical learning: Data mining,
 332 inference, and prediction (2009) Springer, Second Edition.
- 333 7. G. Dong, N.R., Acton, S.T.: Intravital leukocyte detection using the gradient
 334 inverse coefficient of variation. IEEE Transaction on Medical Imaging **24** (2005)
 335 910–924
- 336 8. M. Mirmehdi, X.X., Suri, J.: Handbook of texture analysis (2008) Imperial college
 337 Press.
- 338 9. D. Omerevi, R. Perko, A.T.T.J.O.E., Leonardis, A.: Vegetation segmentation for
 339 boosting performance of msr feature detector. Computer Vision Winter Workshop
 340 (2008) 17–23
- 341 10. Russ, J.C.: The image processing handbook (1995) Third Edition, CRC & IEEE
 342 press.
- 343 11. Y. T. Xi, Z. J. Xiang, P.J.R., Schapire, R.E.: Speed and sparsity of regularized
 344 boosting. 12th International Conference on Artificial Intelligence and Statistics
 345 (AISTATS) **5** (2009) 615–622
- 346 12. Maritz, J.S.: Distribution-free statistical methods (1995) Chapman & Hall, Second
 347 Edition.

- 348 13. van Rijsbergen, C.J.: Information retrieval (1979) Butterworths, London.
- 349 14. Abdou, I.E., Pratt, W.K.: Quantitative design and evaluation of enhancement/
350 thresholding edge detectors. proceedings of the IEEE **67** (1979) 753–763